JTTEE5 14:268-272
DOI: 10.1361/10599630523854
1059-9630/$19.00 © ASM International

Peer Reviewed

New Environmental Barrier Coating System on Carbon-Fiber Reinforced Silicon Carbide Composites

S. Latzel, R. Vaßen, and D. Stöver

(Submitted August 28, 2003; in revised form October 10, 2003)

Carbon-fiber-reinforced silicon carbide composites (C/SiC) are promising materials for high-temperature, light weight structural components. However, a protective coating and environmental barrier coating (EBC) are necessary to prevent the oxidation of the carbon and the reaction of the formed silica scale with water vapor. Current EBC systems use multiple layers, each serving unique requirements. However, any mismatch in the coefficients of thermal expansion (CTE) creates internal stresses and might lead to crack formation. In this case, oxygen and water vapor penetrate through the EBC, reducing the lifetime of the component. Mullite ($Al_6Si_2O_{13}$) is used in many known EBC systems on silicon-based ceramics either as an EBC itself or as a bondcoat. Due to its low CTE and its sufficient thermal cycling behavior, mullite was chosen in this investigation as a first layer. As mullite suffers loss of SiO_2 when exposed to water vapor at high temperatures, an additional protective top coat is needed to complete the EBC system. Different oxides were evaluated to serve as top coat, especially high-temperature oxides with low coefficients of thermal expansion (LCTE). An EBC containing mullite as bondcoat and the LCTE oxide $La_2Hf_2O_7$ as a top coat is proposed. Both layers were applied via atmospheric plasma spraying. In this paper, results of the influence of processing conditions on the microstructure of single mullite and LCTE oxide layers as well as mullite/LCTE oxide systems are presented. Special emphasis was directed toward the crystallinity of the mullite layer and, in the top layer, toward low porosity and reduced crack density.

Keywords atmospheric plasma spraying, C/SiC, ceramic oxide coating, coefficient of thermal expansion, environmental barrier coating, mullite, pyrochlore oxide

1. Introduction

Carbon-fiber-reinforced silicon carbide composites are considered promising materials for high-temperature, lightweight structural components, showing less brittleness than SiC components. Further improvement of the features of these C/SiC composites is intended, but like all carbon-based materials, C/SiC shows significant degradation in air starting at temperatures as low as 400 °C. Uniform oxidation occurs below 800 °C, where oxygen diffuses through cracks; nonuniform oxidation occurs between 800 and 1100 °C, where a protective silica scale forms from the SiC present; and surface oxidation occurs at temperatures above 1100 °C (Ref 1). C/SiC is also very sensitive to the presence of water vapor, by which the oxidation of the SiC matrix is strongly enhanced (Ref 2), and any usually protective SiO_2 scale formed on oxidized SiC surfaces will not be stable, leading to further degradation. For high-temperature application of C/SiC, where water vapor becomes even more aggressive, a protective coating, more accurately an environmental barrier coating (EBC), is needed. Current EBC systems consist of multiple layers, as a single layer cannot fulfill all requirements toward the protection system: erosion protection, oxygen barrier, and water vapor barrier. Additionally, the coating must show specific chemical and physical properties to act as a protection layer. When considering materials for use in EBCs, the coefficient of thermal expansion (CTE) has to be considered closely as any mismatch in the CTE leads to internal stress and consequently to crack formation. Especially in the C/SiC-EBC system, any form of cracks is a potential gateway for oxygen diffusion and has to be avoided. When looking for material suitable for EBC application, mullite is dominant in literature (Ref 3-5). The high creep resistance and the tensile, flexural, and compressive creep behavior of mullite were noted (Ref 6). The CTE of mullite (5.4×10^{-6}/K at 200-1200 °C) delivers a close match to the CTE of SiC (4.5×10^{-6}/K at 200-1000 °C); however, it is considerably larger than the CTE of C/SiC as the content of low CTE carbon fibers in the composite decreases the overall CTE of the composite.

Mullite can act as an EBC itself, but in the presence of water vapor, its silica content volatizes and a porous alumina framework is left on top of the mullite layer (Ref 5). This problem can be solved by adding an extra protective layer on top of the mullite to protect it from water vapor. The requirements of such a top coat are not as high in the field of an oxygen barrier function, as this task is tackled by the mullite layer, but more toward the erosion protection, water vapor barrier, and a close CTE match with the substrate to avoid stresses. Examples of top coats serving EBC purposes are yttrium silicate (Ref 7) and barium strontium alumosilicate (BSAS) (Ref 5, 8), both showing unfavorable characteristics concerning the CTE (anisotropic CTE / different phases with different CTE) and are therefore prone to microcracking.

S. Latzel, R. Vaßen, and **D. Stöver,** Forschungszentrum Jülich GmbH, IWV1, 52425 Jülich, Germany. Contact e-mail: rvassen@fz-juelich.de.

As mullite shows sufficient thermal cycling behavior and has the advantage of being a well-studied EBC material, it was chosen as a first layer in the current study. There are several patents for how to spray crack-free mullite (Ref 9, 10), mainly proposing heating of the substrate while atmospheric plasma spraying. Therefore, the application of this material is rather straightforward, but a top coat is still needed.

One group of high-temperature oxides explored more closely due to the high melting points and the absence of phase transitions is the group of oxides with pyrochlore structure and a low CTE (LCTE pyrochlores). These LCTE pyrochlores are supposed to show a barrier function toward oxygen atoms and water vapor, as the positions of the atoms are rather fixed in the crystal structure. The pyrochlore structure ($A_2B_2O_7 = A_2^{[8]}B_2^{[6]}O_6O'$) is cubic; therefore, no anisotropic behavior concerning thermal expansion is expected.

Lanthanum hafnate is a pyrochlore oxide with a very low CTE (8.2×10^{-6}/K, 200-1200 °C)—to our knowledge, the lowest of all zirconates, hafnates, and stannates with a pyrochlore structure—and was therefore chosen as top layer.

The proposed EBC system therefore consists of a mullite layer and a lanthanum hafnate top layer. This system should protect C/SiC from oxidation and water vapor enhanced corrosion at temperatures ranging from room temperature to considerably higher than 1300 °C.

2. Experimental

Mullite, lanthanum hafnate, and mullite-lanthanum hafnate coatings were produced in a Sulzer Metco (Wohlen, Switzerland) atmospheric plasma spraying (APS) facility with AWV 1-49 mullite powder (Praxair, Wiggensbach, Germany) and Lanthan-Hafnium-Oxide experimental lanthanum hafnate powder (Treibacher Auermet, Treibach-Althofen, Austria) using a Triplex gun. The substrates for testing the influence of the processing conditions on the formation of mullite layer were a 50 × 50 mm plate of SiC (Halsic-R of W. Haldenwanger, Berlin, Germany). An SiC substrate was used as it has a defined CTE (4.5×10^{-6}/K 200-1000 °C), which is similar to the CTE of mullite and therefore effects from CTE mismatch are minimized.

Sandblasted steel plates 50 × 50 mm in size were used as a substrate for lanthanum hafnate layers. Freestanding layers were prepared by removing the steel substrate from the coating with hydrochloric acid.

The substrates for the double coating (mullite layer and a lanthanum hafnate layer) were 30 × 35 mm plates of 2D-C/SiC composite. They were fabricated from high tensile strength carbon fiber fabrics in a modified liquid silicon infiltration process. Details are described in (Ref 11).

The plasma spraying conditions are given in Table 1, with M# for the mullite coatings, L# for the lanthanum hafnate coatings, and DM and DL for the mullite-lanthanum hafnate double coating with DM being the conditions for mullite and DL for lanthanum hafnate, respectively.

Pore-size distributions of the freestanding lanthanum hafnate layers were determined by Pascal 140 and 440 mercury intrusion porosimeters (CE-Instruments, Milan, Italy), operating in a pressure range between 0.0001 and 400 MPa, corresponding to pore diameters between 3.6 nm and 90 μm.

Table 1 Plasma spraying conditions for the investigated coatings

No.	*d*, mm	*v*, m/s	ArC, slpm	Ar, slpm	He, slpm	Rot, %
M1	70	0.5	1.5	20	13	2.5
M2	70	0.75	1.5	20	13	2.5
M3	60	0.5	1.5	20	13	2.5
M4	60	0.75	1.5	20	13	2.5
L1	90	0.5	1.5	20	13	5
L2	90	0.5	2	20	13	5
L3	90	0.5	1.5	15	18	5
L4	70	0.5	1.5	20	13	5
L5	70	0.5	2	15	18	5
DM	60	0.5	1.5	20	13	5
DL	70	0.5	1.5	20	13	5

d, spraying distance; *v*, robot velocity; ArC, carrier gas flux; Ar and He, process gas fluxes; Rot, rotation of the powder feeder (arbitrary units).

The x-ray diagrams were obtained using a Siemens D5000 diffractometer with Cu Kα radiation.

From all samples, optical evaluation of micrographs was performed to study the microstructure and measure the thickness of the different layers, their crack widths, and the crack density of the mullite layer. The crack density was obtained by counting the number of through-thickness cracks intersecting a measuring line in five different cross sections of the layer and normalizating.

3. Results and Discussion

3.1 Mullite Layer

To prepare crack-free, crystalline mullite layers, processing conditions (Table 1, M1-M4) were chosen in a way that mullite was likely to be deposited on the substrate in a crystalline form. The distance from the substrate to the plasma spray gun (spraying distance) and the velocity of the robot holding the plasma spraying gun (robot velocity) were varied to study their influence on the microstructure of the mullite layer.

The mullite layers showed a good level of crystallinity; a typical x-ray diagram is presented in Fig. 1.

On the other hand, when spraying was performed with substrate cooling, i.e., onto a cold surface, the deposition of amorphous material with mullite composition was observed, according to the literature (Ref 12).

All mullite coatings prepared in this paper show segmentation cracks. The typical pattern of segmentation cracks, here on SiC substrate, can be seen in Fig. 2.

All the cracks that were visible on the surface of the layer were through-thickness cracks, as apparent in the optical micrograph Fig. 3. The crack width range is given in Table 2.

The crack size and crack density of M1 and M2 are significantly higher than those of M3 and M4. Both M1 and M2 were sprayed with 70 mm spraying distance, while a 60 mm distance was used for M3 and M4, which both show smaller and less cracks. Within the 60 mm spraying distance samples, M3 and M4, the differences in the range of crack width and in the crack density are equal within the experimental error. The sample with the faster robot velocity, M4, showed slightly lower mean values for the crack width.

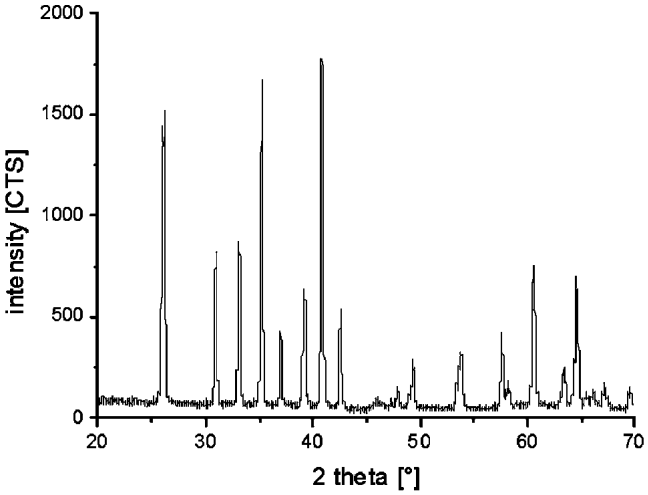

Fig. 1 X-ray diagram of a mullite layer, sprayed with APS condition M1 of Table 1; all peaks can be attributed to mullite.

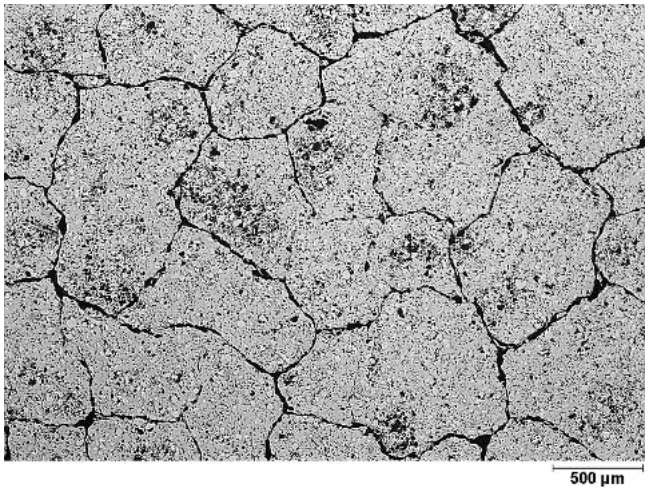

Fig. 2 Optical micrograph perpendicular to the surface of the mullite layer (top view), prepared with APS condition M3 of Table 1, showing the typical pattern of segmentation cracks

However, material with nearly 2 cracks per millimeter showing a width of 2-4 µm cannot be considered as crack-free material. The increase of the robot velocity showed a reduction in crack development; to obtain even fewer cracks the robot velocity can be increased even more. Admittedly, there is no indication that further reduction of the spraying distance and further increase of the robot velocity will produce crack-free mullite layers, but first experiments in the direction of postspraying annealing show promising results toward crack healing in the mullite layer.

The appearance of the segmentation cracks is most likely due to the difference in the coefficient of thermal expansion of the SiC substrate and the mullite layer, although the substrate was specially chosen to show a small CTE mismatch.

This is due to the fact that the coatings are produced at elevated substrate temperatures. This is obtained in the present experiment by coating without substrate cooling. Referring to literature (Ref 12) a sufficiently high temperature would be above the crystallizing temperature of mullite, around 1000 °C. Otherwise amorphous material of mullite composition will be deposited, and later, when the coating is heated above crystallization temperature, mullite will crystallize with a large decrease in volume.

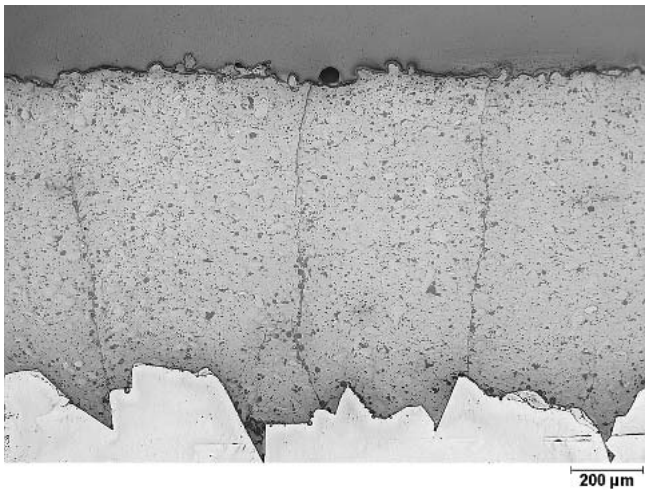

Fig. 3 Optical micrograph of mullite layer prepared with APS condition M4 of Table 1 on SiC substrate (cross-section view) showing through-thickness cracks

Table 2 Mullite layers and corresponding crack width range (crack width, µm) and crack density

Number	Crack width, µm	Crack density, 1/mm
M1	2-30	2.3
M2	10-25	2.9
M3	2-4	1.8
M4	2-4	1.8

For the present experiments, an estimate of the substrate temperature results in 800 °C, which is somewhat below the optimum temperature. If in the plasma spraying process of the mullite layer the substrate is not heated to the optimum temperature, some of the deposited amorphous material may crystallize during the next path of the plasma torch. This mechanism introduces a volume change and hence stresses into the system, which may contribute to the appearance of segmentation cracks.

3.2 Lanthanum Hafnate Layer

Also for the lanthanum hafnate layer, the task was to produce a dense layer. At first, reference spraying parameters were defined (L1 in Table 1). Subsequently, the carrier gas flux, the process gas flux and the spraying distance were varied (L2-L5 in Table 1) and compared with the coating produced with the reference spraying parameter (L1).

A micrograph of the layer sprayed with conditions L1 was used as reference (Fig. 4). This layer exhibits a total cumulative porosity of 17.6%. An overview of the pore-size distribution of the different layers is given in Fig. 5.

When decreasing the spraying distance, the total cumulative

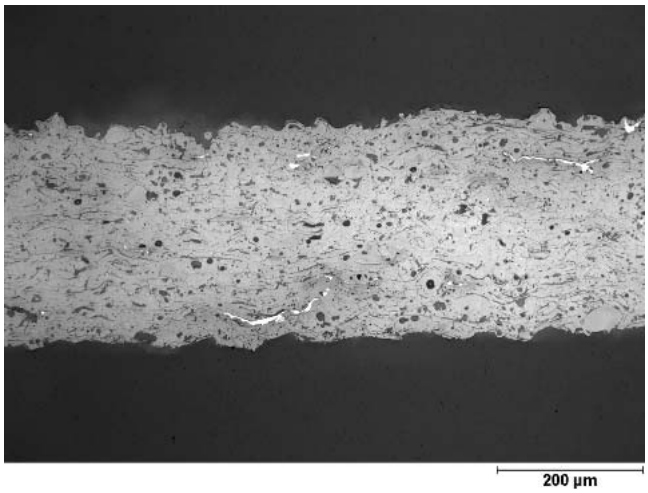

Fig. 4 Micrograph of lanthanum hafnate free standing layer

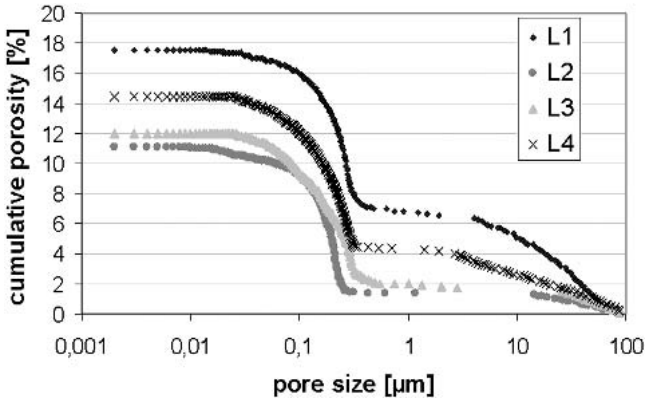

Fig. 5 Pore-size distribution of the investigated lanthanum hafnate layers

porosity decreases from 17.6% for the reference layer L1 to 14.5% for L4. An even further reduction can be observed when the process gas fluxes are changed; here the total cumulative porosity decreases to 12% for L3. The best reduction in porosity is observed when the carrier gas flux is increased (L2). Here, the total cumulative porosity declines to 11%. All the findings can be explained by the fact that the changes in process parameters lead to higher temperatures of the particles when they reach the substrate. The formation of a denser coating is the result.

As all the changes in plasma spraying conditions delivered a decrease in the total cumulative porosity, a sample was prepared, using all of the porosity decreasing processing conditions at the same time (L5). The produced coating shows chipping of the layer and delamination cracks. The porosity was not measurable for this sample. The adhesion between the adjacent spray lamellae was probably not sufficiently high to withstand the larger stresses build up in the denser layer.

The amount of fine pores (1 µm and smaller) does not change significantly with the different plasma spray conditions. These pores have been identified as microcracks in investigations on pore-size distributions elsewhere (Ref 13, 14). The main change

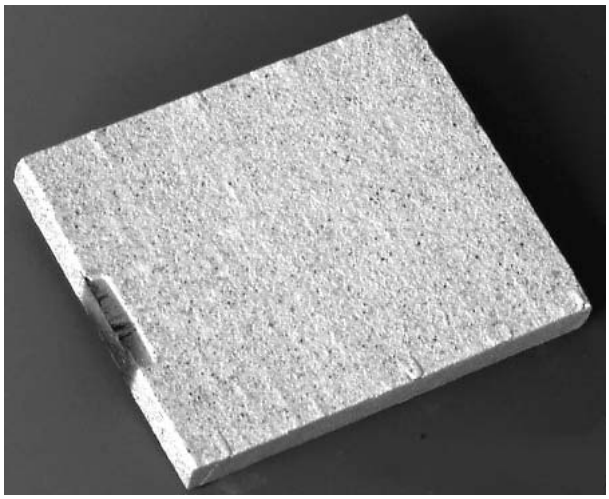

Fig. 6 Photograph of a 30 × 35 mm C/SiC substrate with mullite-lanthanum hafnate double layer coating

is observed in the amount of pores larger than 1 µm. For layer L2 less than 2% of pores are larger than 1 µm, which is a good working base for future variations of the plasma spraying conditions to obtain lower total porosity. Future experiments will be performed on more relevant substrates with low CTE values as SiC or C/SiC as the mismatch in thermal expansion is different from the steel substrates used here. Although the influence on porosity is rather limited for the low deposition temperatures used, there is a significant effect expected during operation at high temperature.

3.3 Double Layer on C/SiC

For the mullite-lanthanum hafnate double layer coatings, the number of cycles of the plasma spray process was decreased to produce thin layers of approximately 100-200 µm for mullite and 50 µm for lanthanum hafnate. Macroscopically, the double coating covers the substrate smoothly (Fig. 6). The atmospheric plasma spraying conditions are given in Table 1 (DM, DL). The resulting mean thickness of the mullite first layer was 149 µm (± 12 µm), and that of the lanthanum hafnate top coat was 54.5 (± 9.5) µm. A micrograph of the double coating is presented in Fig. 7(a) and 7(b).

The adhesion between mullite and the substrate appears good; there are no delamination cracks visible throughout the layer. The adhesion between mullite and the top coat appears ideal; there are no discontinuities and no pores or horizontal cracks visible in the connection zone. However, in the mullite layer, through-thickness cracks are visible. On the position of the underlying cracks, the top coat is disrupted in a way that pores are agglomerated and additional cracks formed. One through-thickness crack can be observed in Fig. 7(a) (top picture) located 1/4 of the way in from the left side.

Therefore, this mullite-lanthanum hafnate double coating is not ideal yet. Special emphasis must be laid on the manufacture of crack-free mullite layer. Approaches will be the use of interlayers, which might result in a certain degree of stress relieve and postspray annealing treatments. Also, the control of the

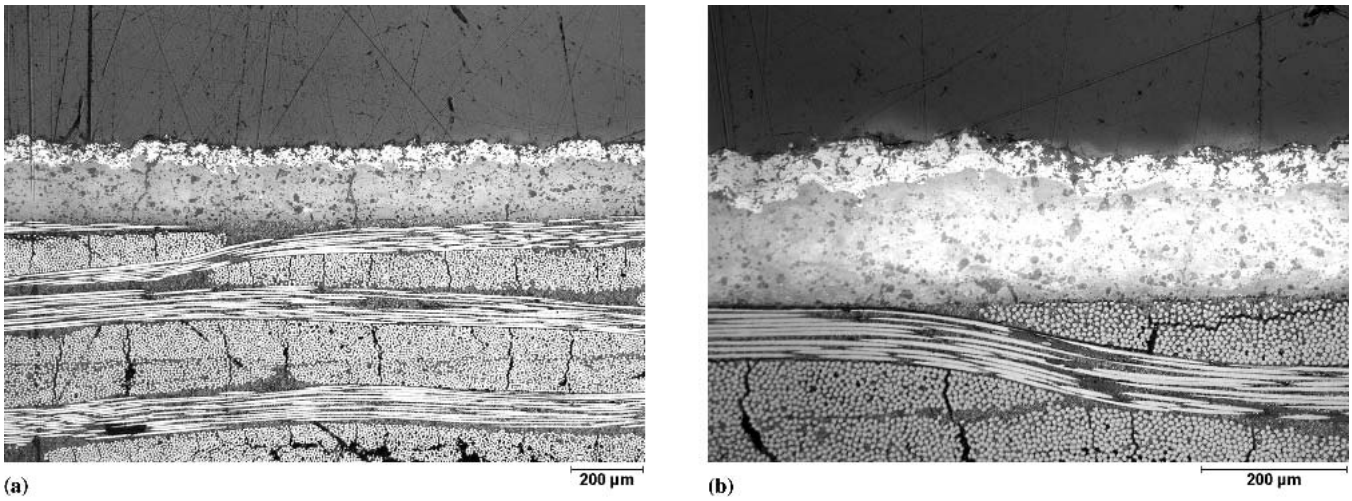

Fig. 7 Optical micrographs of mullite-lanthanum hafnate double coating on C/SiC substrate, different scales.

crysallization of the mullite during spraying might be a parameter to influence the segmentation crack formation. In addition, efforts are directed toward the production of dense top layers, which certainly reduce the need for crack free mullite layers.

4. Summary and Conclusion

Mullite layers were produced by atmospheric plasma spraying to study the influence of processing conditions on the layer. An increase in robot velocity and decrease of spraying distance showed a reduction of segmentation cracks, but a crack-free mullite layer could not be prepared yet. Lanthanum hafnate layers were studied accordingly. A decrease of spraying distance, an increase of carrier gas flux, and a change in process gas fluxes (decrease argon while increasing helium flux) led to a lower porosity, respectively, but a combination of all porosity reducing spraying conditions delivered a strongly cracked, chipped layer.

An EBC coating system on C/SiC was proposed, containing mullite as a first layer and lanthanum hafnate as a top layer. The C/SiC-mullite interface and the mullite-lanthanum hafnate interface of the double layer showed excellent adhesion to each other. As segmentation cracks are still present in the mullite layer, future work will be concentrated both on the production of crack-free mullite coatings and the deposition of dense top layers.

Acknowledgments

The authors would like to thank Mr. Rauwald and Mr. Laufs for performing the plasma-spraying experiments and Mrs. Schwartz-Lückge for the porosity measurements. Also, the XRD measurements by Mr. Lersch are gratefully acknowledged.

References

1. M. Aparicio and A. Durán, C/SiC Composite Materials for Structural Application at Elevated Temperatures. Part 1: Thermodynamic and Chemical Stability, *Bol. Soc. Esp. Cerám. Vidrio,* Vol 39 (No. 6), 2000, p 687-698 (in Spanish)
2. C. Vix-Guterl, C. Grotzinger, J. Dentzer, M.P. Bacos, and P. Ehrburger, Reactivity of a C/SiC Composite in Water Vapour, *J. Eur. Ceram. Soc.,* Vol 21, 2001, p 315-323
3. J.A. Haynes, M.J. Lance, K.M. Cooley, M.K. Ferber, R.A. Lowden, and D.P. Stinton, CVD Mullite Coatings in High Temperature, HP Air-H_2O, *J. Am. Ceram. Soc.,* Vol 83 (No. 3), 2000, p 657-659
4. H. Fritze, J. Jojic, T. Witke, C. Rüscher, S. Weber, S. Scherrer, R. Weiß, B. Schultrich, and G. Borchardt, Mullite Based Oxidation Protection for SiC-C/C Composites in Air at Temperatures up to 1900 K, *J. Eur. Ceram. Soc.,* Vol 18, 1998, p 2351-2364
5. K.N. Lee, Current Status of Environmental Barrier Coating for Si-based Ceramics, *Surf. Coat. Technol.,* Vol 133-134, 2000, p 1-7
6. R. Torrecillas, J.M. Calderón, J.S. Moya, M.J. Reece, C.K.L. Davies, C. Olagnon, and G. Fantozzi, Suitability of Mullite for High Temperature Applications, *J. Eur. Ceram. Soc.,* Vol 19, 1999, p 2519-2527
7. M. Aparicio and A. Duran, Yttrium Silicate Coatings for Oxidation Protection of Carbon-Silicon Carbide Composites, *J. Am. Ceram. Soc.,* Vol 83 (No. 6), 2000, p 1351-1355
8. J.I. Eldridge and K.N. Lee, Phase Evolution of BSAS in Environmental Barrier Coatings, *25th Annual Conference on Composites, Advanced Ceramics, Materials, and Structures,* January 21-27, Cocoa Beach, FL, Ceram. Eng. Sci. Proc. (USA), 2001, Vol 22 (No. 4), p 382-390
9. P.H. McCluskey, H.E. Eaton, D.R. Godin, G.E. Foster, H.D. Harter, S. Chin, G.A. Cotnoir, and C.A. Ellis, Plasma Sprayed Mullite Coatings on Silicon Based Ceramic Materials, US Patent No. 5 869 146, February 9, 1999
10. I.T. Spitsberg, H. Wang, and R.W. Heidorn, Method for Thermally Spraying Crack-free Mullite Coatings on Ceramic-based Substrates, US Patent No. 6 296 909 B1, October 2, 2001
11. M. Müller, J. Mentz, H.-P. Buchkremer, and D. Stöver, Modification of the Liquid Silicon Infiltration Process for C/SiC Production, *26th Annual Conference on Composites, Advanced Ceramics, Materials, and Structures,* January 13-18, Cocoa Beach, FL, Ceram. Eng. Sci. Proc. (USA) 2002, Vol 23 (No. 3), p 339-346
12. K.N. Lee, R.A. Miller, and N.S. Jacobson, New Generation of Plasma-Sprayed Coatings on Silicon Carbide, *J. Am. Ceram. Soc.,* 1995, Vol 78 (No. 3), p 705-710
13. C. Funke, B. Siebert, R. Vaßen, D. Stöver, and J.C. Mailand, Characterization of ZrO_2-7wt.% Y_2O_3 Thermal Barrier Coatings with Different Porosities and FEM Analysis of Stress Redistribution during Thermal Cycling of TBCs, *Surf. Coat. Technol.,* Vol 94-95 (No. 1-3), 1997, p 106-111
14. R. Vaßen, N. Czech, W. Malléner, W. Stamm, and D. Stöver, Influence of Impurity Content and Porosity of Plasma Sprayed Yttria Stabilized Zirconia Layers on the Sintering Behaviour, *Surf. Coat. Technol.,* Vol 141, 2001, p 135-140